CNP/cGMP Signaling Regulates Axon Branching and Growth by Modulating Microtubule Polymerization

Caihong Xia,[1] Minh Nguyen,[1] Amy K. Garrison,[1,2] Zhen Zhao,[1,3] Zheng Wang,[1] Calum Sutherland,[4] Le Ma[1,2,3,5]

[1] Zilkha Neurogenetic Institute, Keck School of Medicine, University of Southern California, Los Angeles, California 90089

[2] Program in Genetic, Molecular and Cellular Biology, Keck School of Medicine, University of Southern California, Los Angeles, California 90089

[3] Neuroscience Graduate Program, University of Southern California, Los Angeles, California 90089

[4] Biomedical Research Institute, University of Dundee, Ninewells Medical School, Dundee, DD1 9SY, United Kindom

[5] Department of Cell and Neurobiology, Keck School of Medicine, Los Angeles, California 90089

Received 4 December 2012; revised 13 February 2013; accepted 13 February 2013

ABSTRACT: The peptide hormone CNP has recently been found to positively regulate axon branching and growth via activation of cGMP signaling in embryonic dorsal root ganglion (DRG) neurons, but the cellular mechanisms mediating the regulation of these developmental processes have not been established. In this study, we provide evidence linking CNP/cGMP signaling to microtubule dynamics via the microtubule regulator CRMP2. First, phosphorylation of CRMP2 can be suppressed by cGMP activation in embryonic DRG neurons, and non-phosphorylated CRMP2 promotes axon branching and growth. In addition, real time analysis of growing microtubule ends indicates a similar correlation of CRMP2 phosphorylation and its activity in promoting microtubule polymerization rates and durations in both COS cells and DRG neuron growth cones. Moreover, direct activation of cGMP signaling leads to increased assembly of dynamic microtubules in DRG growth cones. Finally, low doses of a microtubule depolymerization drug nocodazole block CNP/cGMP-dependent axon branching and growth. Taken together, our results support a critical role of microtubule dynamics in mediating CNP/cGMP regulation of axonal development. Develop Neurobiol 73: 673–687, 2013

Keywords: **axon branching and growth; microtubule dynamics; CNP/cGMP; DRG axons; CRMP2**

INTRODUCTION

Natriuretic peptides are a family of hormones best known for regulating renal sodium and water secretion by binding to receptor guanylyl cyclases and stimulating production of cyclic guanosine monophosphate (cGMP) (Potter et al., 2006). Interestingly, the C-type natriuretic peptide (CNP) was recently

Correspondence to: L. Ma (le.ma@usc.edu).

Contract grant sponsor: Whitehall Foundation (to L.M.), NIH-NINDS (to L.M.), Zumberge Research and Innovation Fund of USC (to L.M.), and the Alzheimer's Research Trust (to C.S.).

Published online 18 February 2013 in Wiley Online Library (wileyonlinelibrary.com).
DOI 10.1002/dneu.22078

found to be required for central afferent bifurcation of dorsal root ganglion (DRG) sensory neurons in the mouse spinal cord (Schmidt et al., 2009; Zhao and Ma, 2009). This novel function depends on the CNP receptor Npr2 and its downstream target, cGMP-dependent protein kinase 1 (PrkG1) (Schmidt et al., 2007; Zhao et al., 2009). In embryonic DRG neuronal culture, activation of CNP/cGMP signaling stimulates axon branching, promotes axon growth, and elicits growth cone turning (Zhao and Ma, 2009; Zhao et al., 2009). Although CNP represents a new class of extracellular factors regulating axonal development, the cellular mechanisms mediating these diverse functions are not known.

Our recent study of DRG axon branching (Zhao et al., 2009) hints that glycogen synthase kinase 3 (GSK3) and its downstream signaling targets may be involved in CNP functions, as GSK-3 can be directly phosphorylated by PrkG1 and perturbation of GSK3 phosphorylation interferes with cGMP-dependent axon branching. GSK3 is also known to regulate neurogenesis, neuronal polarization and axon growth, which all depend on the regulation of microtubule assembly (Hur and Zhou, 2010). Moreover, several microtubule regulators, including collapsin response mediator protein-2 (CRMP2), microtubule associated protein 1B (MAP1B) and adenomatosis polyposis coli protein (APC) are implicated in mediating these functions of GSK3 (Fukata et al., 2002; Zhou et al., 2004; Yoshimura et al., 2005; Kim et al., 2006).

Microtubules are normally bundled in axons but splayed apart in growth cones where they rapidly polymerize and depolymerize in a fashion known as dynamic instability (Lowery and Van Vactor, 2009). This intrinsic property allows dynamic microtubules to explore the intracellular space and is thought to contribute to axon growth and guidance (Mitchison and Kirschner, 1988; Dent and Gertler, 2003; Dent et al., 2011) as well as collateral formation (Gallo, 2011). In fact, inhibition of microtubule dynamics increases growth cone wandering, reduces persistent forward movement, and blocks growth cone turning (Tanaka et al., 1995; Challacombe et al., 1997; Buck and Zheng, 2002; Suter et al., 2004), whereas local stabilization or destabilization of microtubule assembly promotes growth cone attraction or repulsion (Buck and Zheng, 2002). Furthermore, dynamic microtubules are found in nascent branching sites (Dent and Kalil, 2001), and perturbation of their dynamics often interferes with branch formation, albeit with different effects (Letourneau et al., 1986; Baas and Ahmad, 1993; Gallo and Letourneau, 1999; Dent et al., 2004).

Therefore, one of the cellular responses elicited by CNP/cGMP signaling that lead to morphological remodeling in axons could be the modulation of microtubule dynamics. To test this hypothesis, we first investigated phosphorylation of the GSK3 target CRMP2 in DRG neurons. We next used real time imaging to examine microtubule dynamics in COS cells and growth cones of DRG neurons expressing different forms of CRMP2. We further analyzed microtubule response in growth cones challenged by CNP/cGMP activation. Finally, we determined whether CNP/cGMP-dependent DRG axon branching and growth could be blocked by a microtubule inhibitor. Collectively, our results establish a strong connection between microtubule regulation and the novel function of CNP/cGMP signaling in axonal development.

METHODS

Chemicals, Animals, and DNA Constructs

Nocodazole and 8-Br-cGMP were obtained from Sigma (St. Louis, MO). All animal work was done according to protocols approved by the Institutional Animal Care and Use Committees of the University of Southern California following the National Institutes of Health guidelines. Rat embryos were collected from pregnant Sprague Dawley females (purchased from Charles River Laboratories, San Diego, CA) with the plug date designated as embryonic day 0 (E0). The short form of CRMP2 full-length cDNA (Yuasa-Kawada et al., 2003) was cloned by PCR from mouse brain cDNA and then subcloned into a pCAGGS-FLAG expression vector by restriction enzyme digestions. Single amino acid substitution mutants (T514A, T514D) were generated by PCR-based site-directed mutagenesis, and deletion mutants were generated by PCR. All constructs were verified by DNA sequencing as well as by Western blot of proteins expressed in COS cells.

Analysis of CRMP2 Phosphorylation in Neurons by Western Blots

Dissociated DRG neurons (4×10^5 cells/well of six-well plate) were cultured overnight, starved for 3 hr without NGF and stimulated for different times with 50 μM 8-Br-cGMP. Cell lysates were prepared using ice-cold RIPA buffer with protease inhibitors and phosphatase inhibitors. Proteins in the lysate were then separated by SDS-PAGE and transferred onto nitrocellulose membranes, which were probed with the following antibodies: phospho-CRMP2 (Cole et al., 2004, 2006) and mouse anti-tubulin (DM1α). Alexa680- (Invitrogen) and IRDye800-labeled secondary antibodies were used for detection on an infrared imaging system (Odyssey, LI-COR). The quantification was averaged from six individual experiments and compared by the Mann-Whitney test.

In Vitro Branching Assay Using Dissociated DRG Neurons

Dissociated DRG neurons were cultured as previously described (Zhao et al., 2009). Briefly, E14 rat DRG neurons were dissociated and cultured at 8000 cells in 20 μL collagen gels per well and in F12 medium supplemented with N3 and NGF (25 ng/mL). After 24 hr in culture, neurons were treated with CNP (100 n*M*) or 8-Br-cGMP (50 μ*M*). Cells were cultured for additional 24 hr and then fixed for immunostaining with a monoclonal antibody against neurofilament (RMO270, 1:1000, gift from Dr. Virginia Lee, University of Pennsylvania, Philadelphia, PA) and an HRP-conjugated secondary antibody for DAB reaction (Jackson Immunological, ME). In some experiments, nocodazole was added at the same time as CNP and Br-cGMP treatment.

To express various constructs of CRMP2, $\sim 1 \times 10^6$ dissociated DRG cells were electroporated with 2 to 3 μg of plasmid DNA in the Amaxa nucleofector using the reagent and program for rat DRG neurons (Lonza, Germany). After electroporation, cells were diluted with 400 μL of growth medium, incubated at 37°C for 10 min, and then plated together with EGFP-transfected cells (1:1 or 1:2 ratio) at 3–5 $\times 10^4$ cells per 20 μL collagen gels. Cells were cultured for 48 hrs and then fixed for immunostaining using a monoclonal antibody against the FLAG tag (M2, 1:10,000, Sigma).

For quantification, processes extending longer than 20 μm were counted as branches. Total branch numbers were divided by total neuron numbers to obtain average branching points. At least 50 neurons were randomly chosen for measurement in each condition, and each experiment was repeated at least three times. Statistical significance was first determined by one-way ANOVA and then followed by pair-wise Tukey's comparison between the individual experimental condition and the control.

DRG Explant Outgrowth Assay

DRGs were cut into small pieces, plated in collagen gels, and cultured in the presence of NGF (25 ng/mL). CNP and different doses of nocodazole were added to the culture 24 hrs later when the medium was replaced by fresh medium without NGF. DRGs were fixed after another 22 hrs and stained with neurofilament antibodies and Cy3-conjuncted secondary antibodies. Axonal outgrowth (g) between the edge of the explant and the perimeter of the halo was measured at every 45°. To normalize the size variation of explants, an outgrowth index was calculated based on the ratio of outgrowth (g) over the radius (r) of the explant. At least four to six explants were analyzed for each condition. Statistical significance between the control (no nocodazole ± CNP) and other conditions were determined by one-way ANOVA.

Real-Time Analysis of Microtubule Dynamics in Live Cells

To image microtubule ends in neurons, E14 rat DRG explants were electroporated by five 50 ms, 110V square wave pulses using a BTX electroporator with plasmid DNA expressing EB3-GFP (Stepanova et al., 2003). DRG explants were then placed on poly-D-lysine and laminin coated glass coverslips and cultured in the F12/N3 medium with NGF overnight. On the second day, cells on the coverslips were moved to a pre-warmed custom-made stage chamber (32°C) on an Axiovert 200 microscope (Zeiss) and the medium was replaced with fresh F12/N3 supplemented with 10 m*M* HEPES (pH 7.4). The GFP fluorescence was excited by a 100-W mercury lamp attenuated with a neural density filter and 100-ms exposure images were taken using a 63× apochromatic objective (N.A. = 1.4) coupled with a 2.5× optovar and a cooled EMCCD camera (Cascade II, Photometrics) controlled by the Metamorph software (Molecular Devices). To follow microtubules after Br-cGMP or CNP treatment, sequential images at 5 to 10 s intervals were taken for a period of 2 to 4 min at specific time points (every 15 min) after the addition of 50 μ*M* cGMP or 100 n*M* CNP.

To analyze microtubule dynamics in response to CRMP2 overexpression, DRG neurons or COS cells were electroporated or transfected with a bicistronic vector expressing various forms of CRMP2 and EB3-GFP. Fluorescence images were taken 20 hrs later at 5 or 10 s intervals for 2 to 4 min using the same setup described above. To normalize the expression level and the potential changes caused by EB3 expression, we chose cells with similar sized EB3 comets for analysis. To analyze microtubule assembly in response to nocodazole, images were taken 5 min before and then at specific time points after nocodazole addition.

To obtain the rate of microtubule polymerization, EB3 comets were analyzed by the recently developed dCCD method (Garrison et al., 2012) or the plusTipTracker program (Applegate et al., 2011). Polymerization rates were averaged from multiple frames at a single time point for each cell and then presented as mean ± SE of multiple cells analyzed. To obtain the durations, newly-appearing EB3 comets were manually followed frame by frame until they disappeared, and the time intervals were measured between the first and the last frame. EB3-GFP labeled tip length was calculated from the growing ends identified in the dCCD images (Garrison et al., 2012). Most data are normally distributed and the statistical significance was determined by one-way ANOVA followed by Tukey's multiple comparison. For data without normal distribution, the Mann-Whitney test was used.

RESULTS

Phosphorylation of CRMP2 can be Suppressed by cGMP Activation in DRG Neurons

To identify potential cellular mechanisms mediating CNP regulation of axonal development, we first studied CRMP2, a protein that influences microtubule

assembly (Fukata et al., 2002; Yoshimura et al., 2005) and which can be phosphorylated by GSK3 (Cole et al., 2004, 2006; Yoshimura et al., 2005). We asked whether Br-cGMP could modulate CRMP2 phosphorylation at two GSK3 sites (T509/T514) in cultured DRG neurons (Cole et al., 2004, 2006), as these sites have been implicated in axon elongation and neuronal polarity (Cole et al., 2004; Yoshimura et al., 2005). As shown by Western blotting using a T509/T514-specific phospho-antibody [Fig. 1(A)], the phosphorylation level of CRMP2 at these two sites started to decrease after treating the cells with Br-cGMP for 15 min and reached ~25% reduction after 1 hr exposure [Fig. 1(B)]. A similar change was also observed in DRG neurons treated with CNP (data not shown). Thus, the biochemical analysis suggests CRMP2 as a downstream target of CNP/cGMP signaling in DRG neurons.

Phosphorylation-Dependent Promotion of Axon Branching and Growth by CRMP2

To test the role of CRMP2 and it phosphorylation in axon branching and growth, we next overexpressed CRMP2 in dissociated DRG neurons and examined axonal morphology without activating CNP/cGMP signaling. To normalize the potential variation of culture conditions, DRG neurons were electroporated separately with DNA constructs of FLAG-tagged CRMP2 or EGFP and then cultured together in collagen gels. Two days after transfection, neurons stained positive for wild-type (WT)-CRMP2 displayed more branches than those expressing EGFP in the same culture [Fig. 2(A)]. The branch distribution for WT-CRMP2 showed a significant right-shift over EGFP controls [Fig. 2(H)], and more than 70±10% WT-CRMP2-positive neurons had two or more branches, as compared with 35 ± 10% EGFP-expressing cells. In addition, the average number of branching points increases from 1.40 ± 0.07 per neuron for EGFP-expressing cells to 2.35 ± 0.09 by for WT-CRMP2-expressing cells [Fig. 2(I)].

We then tested the dependence of this branching activity on CRMP2 phosphorylation at the T514 site. We chose to focus on this site because it is critical to mediating GSK3-depenent neuronal polarity and tubulin binding (Yoshimura et al., 2005). Two phospho-mutants were overexpressed in DRG neurons [Fig. 2(B–G)]. One is the T514A mutant (T514-CRMP2) that mimics the unphosphorylated active state by blocking its phosphorylation with a substitution of threonine by alanine; and the other is T514D, which mimics the phosphorylated form that is unable to interact with tubulin heterodimers (Fukata et al., 2002). As shown in Figure 2(H), the overall branch distribution significantly shifted to the right in T514A-CRMP2 overexpressed neurons, while the distribution for T514D-CRMP2 cells shifted only slightly. As a result, 84 ± 13% T514A-CRMP2-expressing neurons had two or more branches, while only 38 ± 17% EGFP-expressing neurons and 54 ± 9% T514D-positive cells did. The average number of branching points in T514A-CRMP2 neurons increased significantly (~2.1×) to 2.93 ± 0.14 per neuron from that of the control neurons. In contrast, T514D-CRMP2-positive cells had 1.3x more branches (1.83 ± 0.10 per cells) than the control cells [Fig. 2(I)], likely due to incomplete inhibition of CRMP2 activity by the mutant that retains an intact T509 site. Nonetheless, these results indicate that the branching activity depends on the phosphorylation state of CRMP2.

We also measured axon growth in dissociated DRG neurons overexpressing CRMP2 [Fig. 2(J)]. Normally, the basal level of axonal length, defined by the longest neurite, was 214 ± 12 μm. Overexpression of WT- or T514A-CRMP2 led to a small but significant increase of axon length to 257 ± 13 μm and 269 ± 10 μm, respectively. However, overexpression

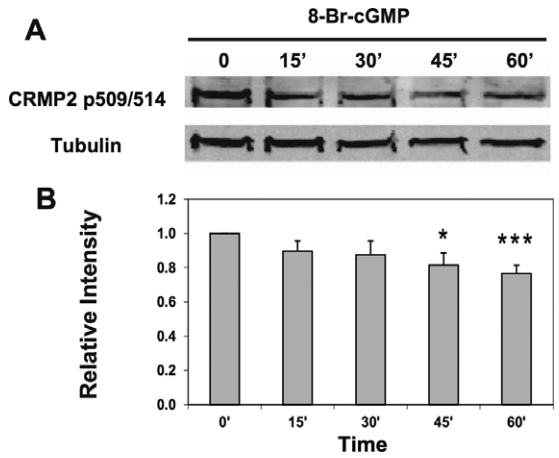

Figure 1 Phosphorylation of CRMP2 at T509/T514 is regulated by cGMP signaling. A) Dissociated E14 rat DRG were starved for 3 hrs and then stimulated with 50 μM Br-cGMP for the time period indicated. Phosphorylation of CRMP2 at T509/T514 was analyzed by Western blot with a specific phosphoantibody. As a loading control, tubulin was probed on the same blot. B) The relative phosphorylation level is plotted as an average of the normalized ratio (mean ± SE) of pCRMP2/tubulin from six different cultures and shows a small but significant reduction after 45 min as compared with 0 min (**$p < 0.01$, *$p < 0.05$, Mann-Whitney test).

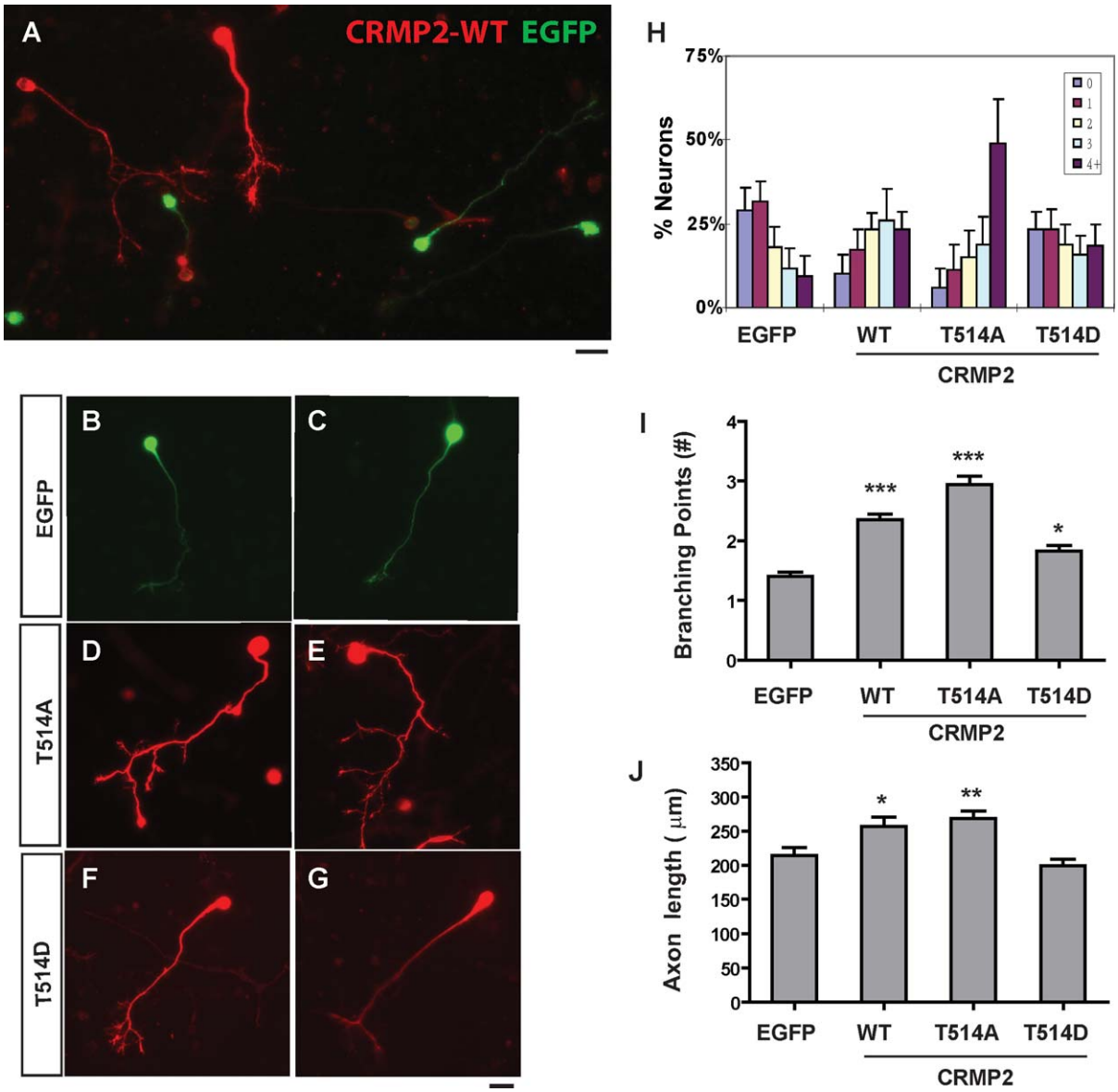

Figure 2 CRMP2 over-expression in DRG neurons enhances axonal branch formation. A) Dissociated DRG neurons were transfected with wild type (WT) CRMP2-FLAG and EGFP separately, and then mixed together and cultured in collagen gels for 48 hr. CRMP2 expression was detected by staining with a FLAG antibody and Cy3-conjugated secondary antibodies (red) and EGFP was detected by its own fluorescence (green). Note the increase in branches in CRMP2-expressing neurons but not in EGFP cells. Scale bar: 20 μm. B–G) Representative images of dissociated DRG neurons that were transfected with EGFP (B, C), T514A (D, E) or T514D (F, G) of FLAG-tagged CRMP2 and cultured in collagen gels for 48 hr. Scale bar: 20 μm. H, I) Comparison of axon branching by the distribution of neurons with a different number of branches (H, mean ± STD) or by the average number of branching points (I, mean ± SE) measured from neurons transfected with plasmids expressing EGFP, WT, T514A, or T514D of CRMP2-FLAG. Both WT and T514A showed increased branch formation (***$p < 0.001$, **$p < 0.01$, ANOVA with Tukey's comparison). J) Comparison of axonal length (defined as the longest neurites, mean ± SE) of dissociated DRG neurons transfected with different plasmids (***$p < 0.001$, *$p < 0.05$, ANOVA).

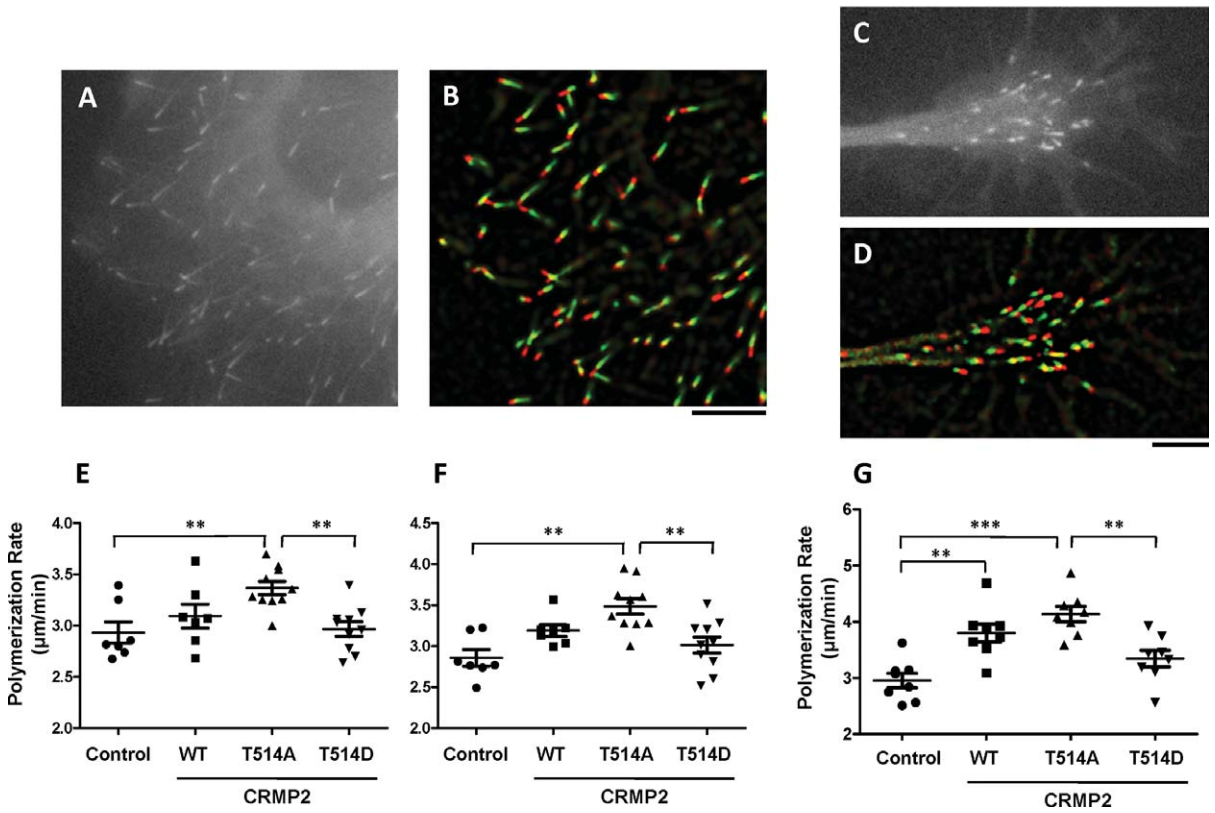

Figure 3 Over-expression of CRMP2 promotes microtubule polymerization rates in COS cells and DRG neuron growth cones. A–D) Microtubule assembly was analyzed by following EB3-GFP labeled plus-ends in COS cells (A) or DRG growth cones (C). Labeled ends were color coded and then analyzed by the dCCD method (B and D). Scale bars: 5 μm. E–G) Comparison of microtubule polymerization rates (mean ± SE) in COS cells (E, F) or in DRG growth cones (G) expressing EB3-GFP alone or with different forms of CRMP2 from a bicistronic vector. Polymerization rates were calculated from single growing microtubule ends using the dCCD method (E, G) or by the plusTipTracker program (F). In both COS cells and DRG growth cones, significant increases (p values from ANOVA are 0.0028 (E), 0.0004 (F), and <0.0001 (G)) were found in cells expressing T514A of CRMP2 when compared with the control cells expressing EB3-GFP alone or with T514D-CRMP2 based on Tukey's multiple comparisons (**$p < 0.01$, ***$p < 0.001$). Note that WT-CRMP2 also caused significant increase in microtubule polymerization rates as compared with the EB3-GFP control in growth cones.

of the T514D mutant resulted in a slight reduction of axonal length to 199 ± 10 μm, which is not statistically different from that of the control neurons. These results are consistent with the previous findings obtained from cultured hippocampal neurons (Fukata et al., 2002) and thus suggest CRMP2 as a likely cellular mediator for CNP/cGMP signaling in DRG axon growth and branching.

Phosphorylation-Dependent Regulation of Microtubule Polymerization by CRMP2 in COS Cells and DRG Growth Cones

As CRMP2 is known to promote microtubule assembly in cells (Fukata et al., 2002), we hypothesize that it mediates CNP-dependent axon growth and branching by modulating microtubule dynamics. However, the exact site of microtubule regulation is not known, as none of the dynamic parameters has been measured in the presence of activated CRMP2. Thus, we made a bicistronic construct that co-expressed different forms of CRMP2 along with EB3-GFP. As EB3-GFP binds preferentially to the growing plus-end of microtubules (Stepanova et al., 2003), we could use a recently developed dual color-coded display (dCCD) method (Garrison et al., 2012) to rapidly measure microtubule polymerization rates in the entire cell [Fig. 3(A,B)].

We first measured polymerization rates in COS cells cultured at 32°C and compared the rates

Table 1 Summary of the Rates (Mean ± SE) of Microtubule Polymerization (μm/min) in COS Cells and Growth Cones of DRG Neurons Expressing Different Forms of CRMP2

	COS Cells		DRG Growth Cones
	dCCD	plusTipTracker	dCCD
Control	2.93 ± 0.10 (7)	2.86 ± 0.10 (7)	2.96 ± 0.13 (8)
CRMP2-WT	3.09 ± 0.12 (7)	3.19 ± 0.07 (7)	3.80 ± 0.16 (8)
CRMP2-T514A	3.38 ± 0.06 (10)	3.49 ± 0.09 (10)	4.12 ± 0.14 (8)
CRMP2-T514D	2.97 ± 0.07 (10)	3.01 ± 0.10 (10)	3.34 ± 0.15 (8)

Numbers in the parentheses indicate the number of cells or growth cones analyzed for each condition.

between cells expressing WT, T514A, or T514D-CRMP2 as well as those expressing EB3-GFP alone. The rates calculated during a 2-min period [Fig. 3(E)] increased from 2.93 ± 0.10 μm/min in the control cells to 3.38 ± 0.06 μm/min in cells expressing T514A proteins. Interestingly, neither the phosphorylated mutant (T514D) nor the WT-CRMP2 elicited any significant change (Table 1), indicating that microtubule regulation depends on the state of CRMP2 phosphorylation. To confirm the observation based on the analysis by the dCCD method, we used an automated tracking program plusTipTracker (Matov et al., 2010) to measure the rates from the same set of images (Table 1). Again, we found similar correlation of polymerization rates and phosphomutants of CRMP2 as the rates differ significantly between T514A-expressing cells and control or T514D-expressing cells [Fig. 3(F)].

To test whether the rate-promoting activity found in COS cells also applies to neurons, we used the same experimental strategy and the dCCD method to measure microtubule polymerization rates from dynamic microtubules in the growth cone of DRG neurons. In neurons expressing EB3-GFP alone, the rate was 2.96 ± 0.13 μm/min (Table 1). However, T514A-CRMP2 caused significant increase of the rates by 39% to 4.12 ± 0.14 μm/min, while the phosphorylation-mimicking mutant (T514D) had less effect (3.34 ± 0.15 μm/min, 13% increase) [Fig. 3(L), Table 1). More importantly, the rate difference between T514A- and T415D-neurons is consistent with that found in COS cells and demonstrates an important role for non-phosphorylated CRMP2 in promoting microtubule dynamics. Interestingly, we also found that overexpression of WT-CRMP led to a significant increase of the rate in growth cones [28%, Fig. 3(L), Table 1], indicating different responses between DRG neurons and COS cells.

We also measured the durations of microtubule polymerization by following the appearance and the disappearance of EB3-GFP labeled ends in COS cells and DRG growth cones. Like the rates, we found a similar change in COS cells measured over a period of 4 min [Fig. 4(A)], increasing from 49.94 ± 2.84 s in the control cells to 72.82 ± 5.15 s in cells expressing T514A, but not in T514D-cells (49.57 ± 2.57 s) (Table 2). A similar increase was also found in DRG neuron growth cones. Twenty hours after transfection, T514A-CRMP2 increased the durations by 36% to 99.22 ± 5.48 s from 65.22 ± 3.38 s in the control growth cones [Fig. 4(B), Table 2]. In both cases, WT-CRMP2 also led to significant duration increase by ∼30% to 66.10 ± 4.71 s and 86.90 ± 4.60 s respectively.

Thus, these results reveal an important function of CRMP2 phosphorylation in regulating microtubule dynamics in intact cells and demonstrate a nice correlation with its activity in axon branching and growth (Fig. 2).

CNP/cGMP Activation Modulates Microtubule Assembly Dynamics in DRG Neuron Growth Cones

To test whether microtubule assembly is indeed a target of CNP/cGMP signaling, we next examined EB3-GFP-comets in DRG neuron growth cones challenged by Br-cGMP or CNP [Fig. 5(A,B)]. We first measured the polymerization rates using the dCCD method and compared the data pooled from several experiments. We calculated the ratio of the rates measured after stimulation over the initial rates (at 0 min) in the same growth cone and compared the ratio between control and CNP/cGMP-activated growth cones [Fig. 5(C)]. A modest but significant increase (8%, $p = 0.008$, t-test, $n = 11$) was found 15 min after the addition of Br-cGMP or CNP to the culture medium, at a time when CRMP2 phosphorylation starts to decrease (Fig. 1). This increase persisted for at least 30 min when the rates were analyzed at 30 min and 45 min after activation [Fig. 5(C)]. However, it was not observed in control growth cones, indicating that the increase observed above is specific for CNP/cGMP activation. In addition, the same rate increase was observed when the rates were analyzed by tracking EB3-GFP labels manually (data not shown).

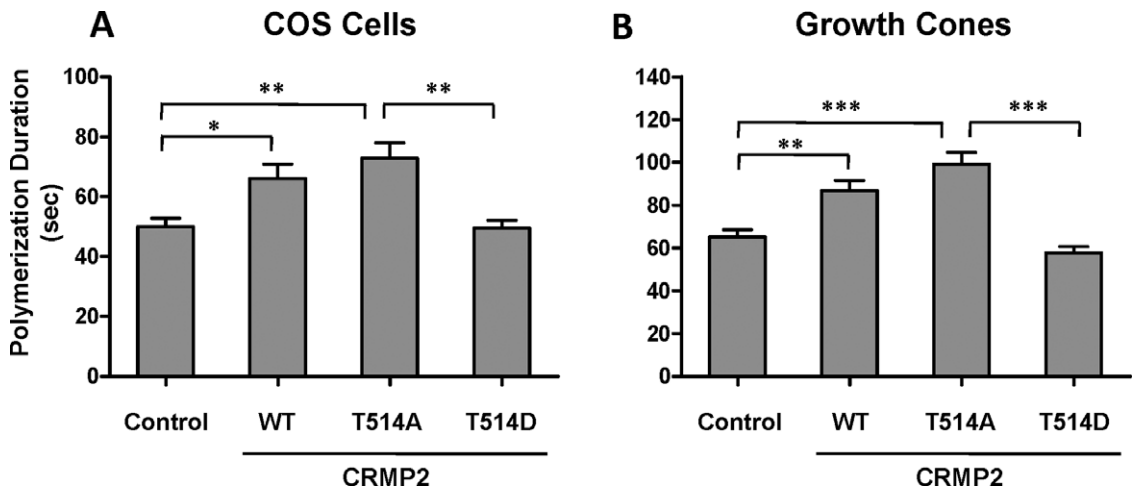

Figure 4 Overexpression of CRMP2 promotes microtubule polymerization durations in COS cells and DRG neuron growth cones. Comparison of microtubule polymerization durations (mean ± SE) in COS cells (A) or in DRG growth cones (B) expressing EB3-GFP alone or with different forms of CRMP2 from a bicistronic vector. Significant differences (ANOVA) are found in cells expressing WT or T514A of CRMP2 when compared with control cells expressing EB3-EGFP alone or CRMP2-T514D based on Tukey's multiple comparisons (*$p < 0.05$, **$p < 0.01$, ***$p < 0.001$).

Next, we measured polymerization durations in the growth cones challenged by Br-cGMP and found they were increased by nearly 30% [Fig. 5(D]. The increase started at 15 min and persisted for the next 30 min. Taken together, microtubule assembly in DRG neurons is greatly enhanced after cGMP activation as a result of increased microtubule dynamics, which is consistent with the data obtained for CRMP2 above (Figs. 3 and 4).

Low Doses of Nocodazole Inhibit CNP/cGMP-Dependent Axon Branching in DRG Neurons

To test whether increased polymerization rates from dynamic microtubules is required for CNP/cGMP-dependent axonal development, we examined the effect of a microtubule depolymerizing drug nocodazole on DRG axon branching in culture, as low doses of nocodazole have been used to block dynamics but not overall microtubule assembly (Tanaka et al., 1995; Rochlin et al., 1996; Gallo and Letourneau, 1999; Dent et al., 2004).

Table 2 Summary of the Durations (Mean ± SE) of Microtubule Polymerization in COS Cells or DRG Neurons Expressing Different Forms of CRMP2

	COS Cells	DRG Growth cones
Control	49.94 ± 2.84 (25)	65.22 ± 3.38 (31)
CRMP2-WT	66.10 ± 4.71 (31)	86.90 ± 4.60 (29)
CRMP2-T514A	72.82 ± 5.15 (23)	99.22 ± 5.48 (29)
CRMP2-T514D	49.57 ± 2.57 (23)	57.71 ± 2.88 (24)

Numbers in the parentheses indicate the number of cells, growth cones, or axons analyzed for each condition.

To first confirm the inhibition of microtubule dynamics, we used the dCCD method to analyze EB3-GFP labeled microtubule ends in COS cells [Fig. 6(A–D)]. We found that microtubules remained dynamic after the treatment with low doses of nocodazole, but the polymerization rates decreased within 10 min and persisted at the reduced rates for at least 30 min. The reduction was 18 ± 4% at 33 n*M* nocodazole, but became more profound and reached ~35 ± 6% at 100 n*M* nocodazole [Fig. 6(E)]. The rate reduction appears to correlate well with that of the EB3-GFP labeled tip length, which exhibited similar time- and dose-dependent reduction [Fig. 6(F)]. Thus, consistent with previous studies (Vasquez et al., 1997; Jaworski et al., 2009), low doses of nocodazole can be used to perturb microtubule dynamics without disassembling microtubule networks.

Following the dose analysis in COS cells, we next tested the effect of nocodazole on DRG neurons at concentrations between 0 and 100 n*M*. These neurons normally displayed simple morphology after two days of culture in collagen gels, with 28 ± 7% (mean ± STD) of neurons having no branches, 36 ± 7% having one branch, 21v5% having two, and less than 15% having three or more branches [Fig. 7(A,I)]. As previously reported (Zhao and Ma, 2009), including CNP in the culture in the last 24 hr resulted

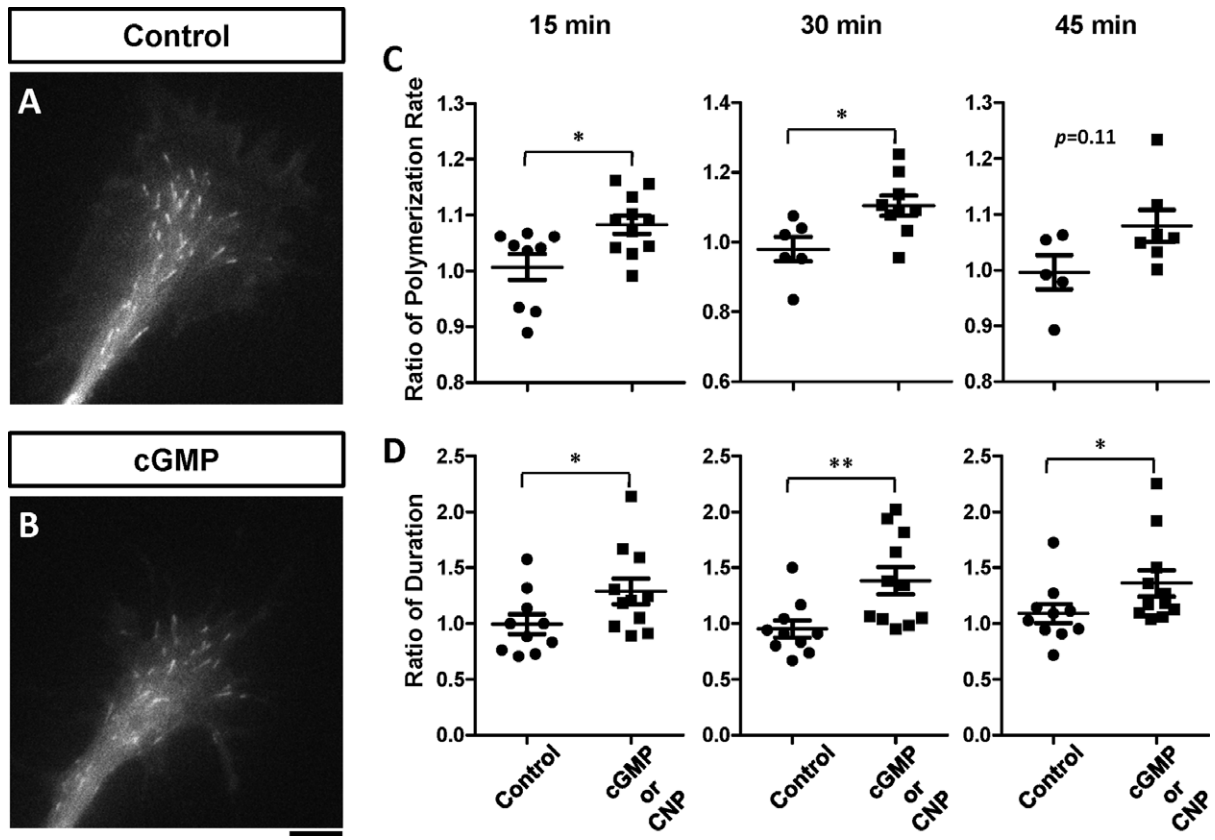

Figure 5 CNP or cGMP activation promotes microtubule assembly in DRG neuron growth cones. A, B) Microtubule assembly was analyzed in the growth cones of EB3-GFP-expressing DRG neurons that were treated without (A) or with 50 μ*M* Br-cGMP (B). Scale bar: 5 μm. C) Microtubule polymerization rates in growth cones were calculated by the dCCD method and plotted as the ratios between those at time 15', 30, or 45' after stimulation and those at time 0'. The rate ratios are close to one in control growth cones ($n > 5$), but increased significantly in growth cones ($n > 7$) treated with 50 μ*M* Br-cGMP or 100 n*M* CNP (*$p < 0.05$, **$p < 0.001$, Mann-Whitney test). D) Durations of microtubule polymerization in growth cones were calculated and plotted as the ratio between those at time 15', 30, or 45' and those at time 0'. The duration ratios are close to one in control growth cones ($n = 10$), but has >20% increase in growth cones ($n = 11$) treated with 50 μ*M* Br-cGMP (*$p < 0.05$, **$p < 0.001$, Mann-Whitney test).

in >71% of neurons developing more than two branches [Fig. 7(E)]. As a consequence, the average branching number per cell is increased from 1.30 ± 0.09 to 2.32 ± 0.04 [mean ± SE, Fig. 7(K)]. However, the addition of nocodazole simultaneously with CNP treatment reduced this increase and returned it to the control level in a concentration-dependent manner. With increasing nocodazole concentrations, the distribution of neurons with different number of branches shifts toward the left [Fig. 7(J)], indicating a negative effect on branching. At 10 n*M* nocodazole, 69 ± 16% (mean ± STD) of CNP-treated neurons had more than two branches, while at 33 n*M* and 100 n*M*, the percentage was lowered to 46 ± 18% and 14 ± 15%, respectively [Fig. 7(F–H,J)]. The change in distribution can be also demonstrated by the decrease in the average branching point, which was lowered to 1.94 ± 0.09, 1.20 ± 0.05 and 0.70 ± 0.04 per neuron at these three concentrations respectively. As a comparison, nocodazole also reduced the basal level of branching [Fig. 7(B–D,K)]: in the presence of 10 n*M* nocodazole, the average branching point was 1.10 ± 0.08 per cell, while at 33 n*M* and 100 n*M*, it declined to 0.76 ± 0.02 and 0.39 ± 0.07 per cell, respectively.

We also tested the nocodazole effect on Br-cGMP-treated DRG neurons and obtained similar results, as nocodazole at 10 to 100 n*M* inhibited axon branching of Br-cGMP-treated neurons [Fig. 7(L)]. Furthermore, to exclude the secondary effect of nocodazole on axon growth, we normalized the branching number to the length of the main axons. Again, we found

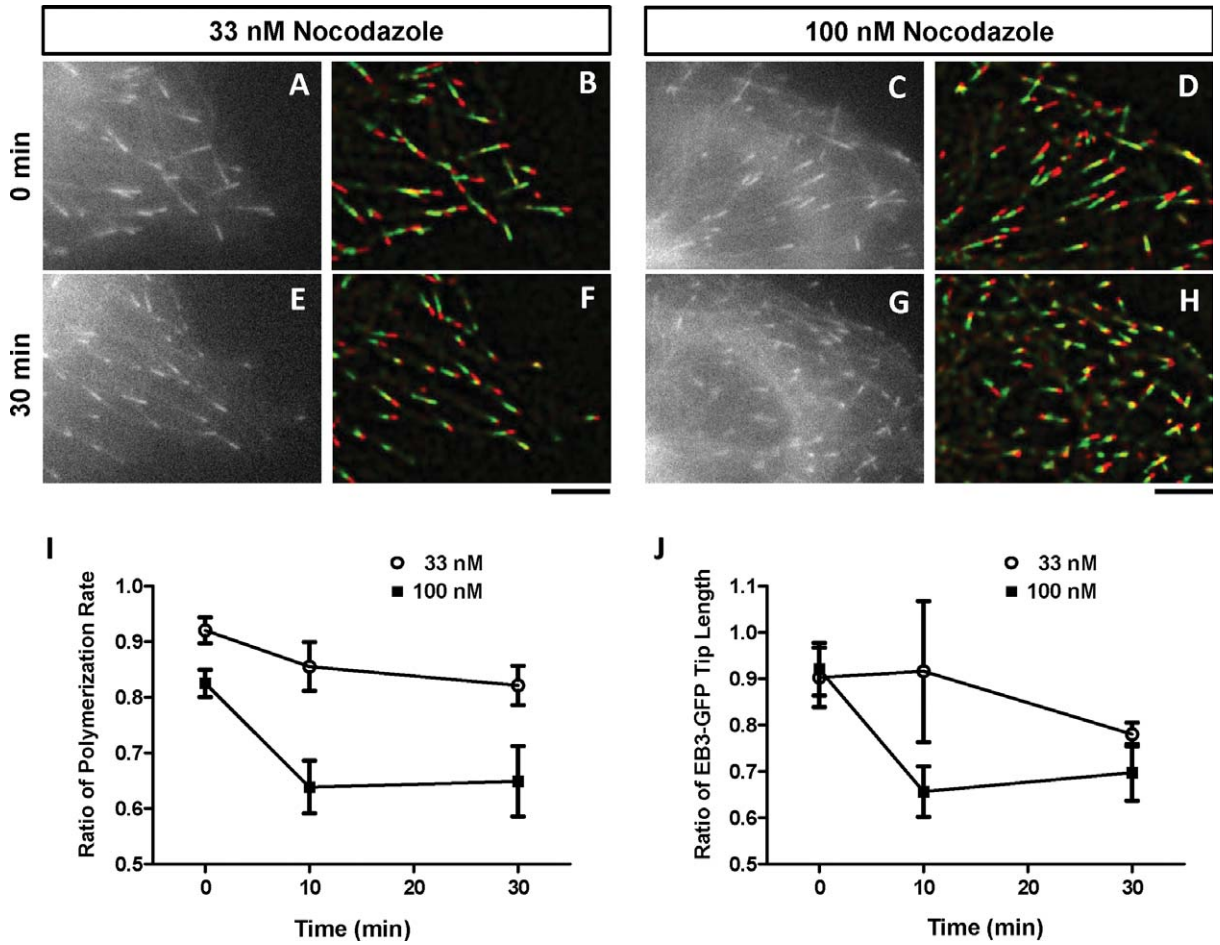

Figure 6 Low doses of nocodazole affect microtubule dynamics in COS cells. A–H) Analysis of microtubule assembly in EB3-GFP-expressing COS cells (A, C, E, G) challenged by nocodazole at two low doses (33 n*M* or 100 n*M*). EB3-GFP labeled microtubule plus-ends were imaged at 0 min (A–D) or 30 min (E–H) after nocodazole treatment, and then analyzed by the dCCD method (B, D, E, H) to calculate polymerization rates and EB3-GFP labeled tip length. Scale bar: 5 μm. I, J) Comparison of microtubule polymerization rates or EB3-GFP labeled tip length in COS cells treated with different doses of nocodazole. Both parameters were calculated and plotted as the ratio between the values obtained at different time points after nocodazole treatment and those obtained 5 min before treatment. For both parameters, 100 n*M* nocodazole led to stronger reduction as compared with 33 n*M*.

a dose-dependent reduction of both CNP and Br-cGMP-stimulated branching [Fig. 7(M,N)], indicating that this inhibition on axon branching is direct. Thus, our pharmacological study demonstrates that dynamic microtubules are required for CNP/cGMP-dependent axon branching of DRG neurons.

CNP-Stimulated Axon Growth can be Attenuated by Nocodazole

Since our previous study had shown that CNP could stimulate axon growth in DRG explant culture (Zhao and Ma, 2009), we tested whether this positive effect could also be blocked by nocodazole. Consistent with our previous study, addition of CNP to DRG explants leads to increased axon growth, with longer and denser axons surrounding the explant (Fig. 8). This effect can be quantified and compared by the outgrowth index, which increased from 2.30 ± 0.11 (mean $\pm$ SE) in the untreated explants to 3.36 ± 0.09 in the CNP-treated explants [Fig. 8(I)]. However, addition of nocodazole to the culture at the same time of CNP treatment blocked this increase in a dose-dependent manner. The minimum effective nocodazole concentration was 33 n*M*, at which the axons at the periphery of the explants were less dense, and the

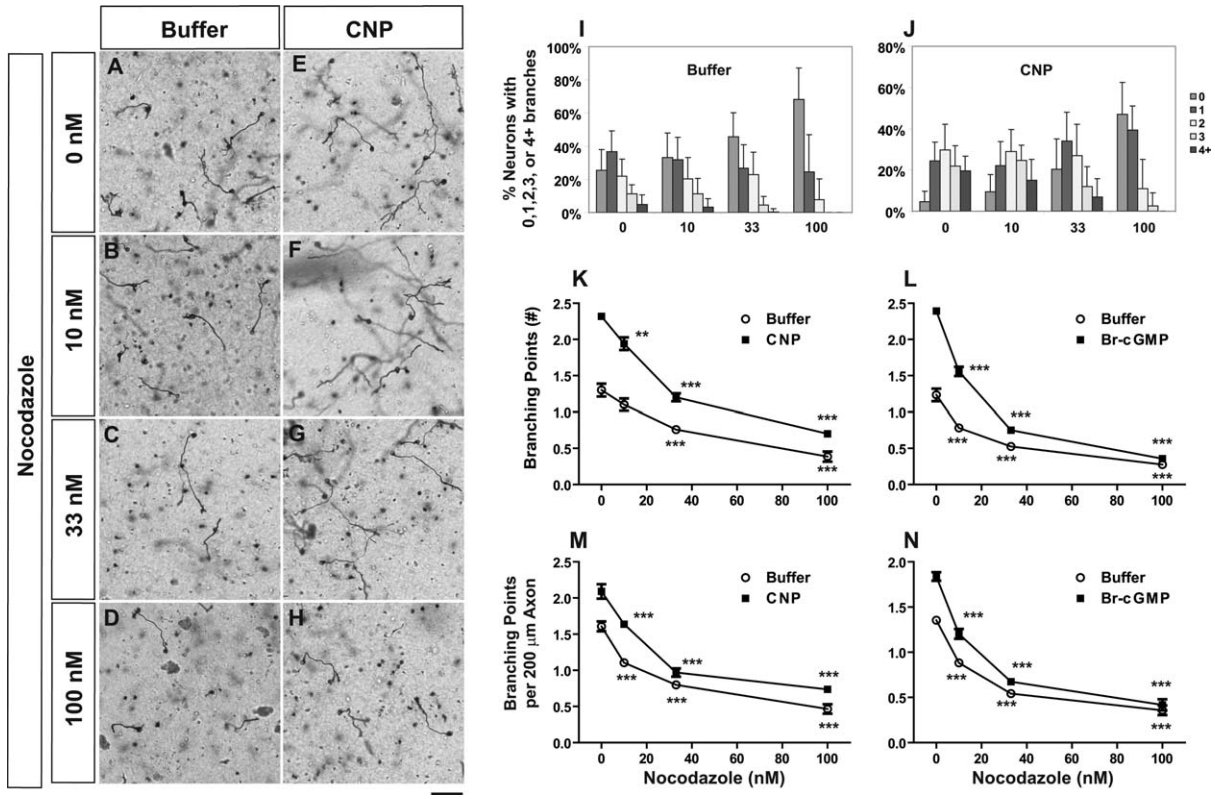

Figure 7 Low doses of nocodazole block CNP/cGMP-dependent axon branching in dissociated DRG culture. A–H) Dissociated DRG neurons were cultured in collagen gels for 24 hr and then treated with different concentrations of nocodazole in the presence of buffer (A–D) or 100 n*M* CNP (E–H). Cells are visualized by HRP staining with a neurofilament antibody. Scale bar: 100 μm. I–N) Comparison of axon branching by the distribution of neurons (mean ± STD) with different numbers of branches (I, J), or by the average number (mean ± SE) of branching points (K, L) or branching points per 200 μm axon length (M, N) measured from neurons cultured with buffer as controls (I), 100 n*M* CNP (J, K, M) or 50 μ*M* Br-cGMP (L, N) under different nocodazole concentrations. Significance is shown for samples that are different from the corresponding 0 n*M* nocodazole samples (**$p < 0.005$, ***$p < 0.001$, ANOVA with Tukey's comparison).

outgrowth index decreased to 2.46 ± 0.10. Interestingly, the same concentration of nocodazole reduced the basal level growth from 2.30 ± 0.11 to 1.40 ± 0.12. At the highest dose tested (100 n*M*), nocodazole reduced the basal growth to 1.03 ± 0.05 and the CNP-induced growth to 1.96 ± 0.03. Thus, these results demonstrate the importance of microtubule assembly in both basal and CNP-stimulated axon growth of DRG neurons.

DISCUSSION

CNP/cGMP signaling provides a novel mechanism that guides axons to connect with proper targets during development. Following the recent identification of this pathway in regulating axon branching, growth, and guidance (Schmidt et al., 2007, 2009; Zhao and Ma, 2009; Zhao et al., 2009), we provide biochemical, cell biological and pharmacological data to link this signaling pathway to downstream regulation of microtubule polymerization (Fig. 9).

First, we show that the microtubule regulator CRMP2 is a downstream target of CNP/cGMP signaling. Our previous study has identified GSK3 as a modulator of cGMP-dependent branching (Zhao et al., 2009), and now we extend this finding to CRMP2, one of the GSK3 substrates that is known to regulate neuronal polarization, axonogenesis, axon growth and branching (Inagaki et al., 2001; Fukata et al., 2002; Yuasa-Kawada et al., 2003; Yoshimura et al., 2005). Here, we show that the CRMP2 phosphorylation at two of the GSK3 sites is reduced by cGMP activation in DRG neurons [Figs.1 and 9(A)]. The change follows a time course that mirrors that

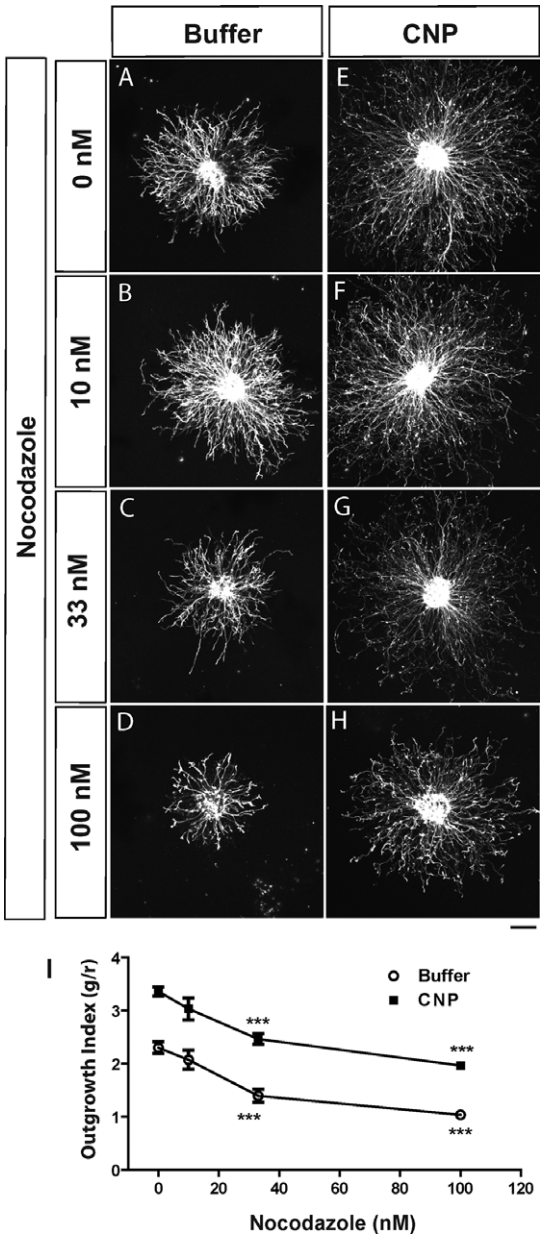

Figure 8 Low doses of nocodazole block CNP-stimulated axon growth from DRG explants. A–H) DRG explants were cultured in collagen gels for 24 hr and then treated with different concentrations of nocodazole in the absence (A–D) or presence (E–H) of 100 n*M* CNP. Cells were fixed and stained with a neurofilament antibody and a fluorescently labeled secondary antibody. Scale bar: 200 μm. I) Comparison of axon growth by the outgrowth index (g/r, mean ± SE), which is calculated by the ratio of outgrowth (g) over diameter (r) of each explant. Significance is shown for samples that are different from the controls with 0 nM nocodazole (***$p < 0.001$, ANOVA).

of GSK3 phosphorylation (Zhao et al., 2009). In addition, overexpression of different phosphorylation forms of CRMP2 led to consistent effects on DRG axon branching and growth. These results are consistent with the disinhibition model in which CNP/cGMP activation leads to GSK3 phosphorylation, hence relieving CRMP2 from the inactive phosphorylated state (Kim et al., 2006; Zhao et al., 2009).

In addition, our live cell imaging study supports the notion that regulation of microtubule dynamics results from the activation/inactivation of this signaling pathway. Using EB3-GFP to analyze microtubule dynamics, we find that CRMP2 stimulates polymerization rates and durations in both COS cells and DRG neuron growth cones, and demonstrate its dependence on phosphorylation state [Figs. 4 and 9(A)]. By comparing the measurement in response to CNP/cGMP activation, we also demonstrate that activation of cGMP signaling leads to ~8% rate increase and 30% duration increase in growth cones (Fig. 5, Tables 1 and 2). This increase in microtubule dynamics induced by a positive cue is consistent with the opposite change elicited by a negative extracellular cue, Sema3A (Dent et al., 2004). Thus, our data clearly point to the sites of microtubule dynamics that can be regulated by CNP and demonstrate a mechanism that is shared by other extracellular cues.

Finally, we provide pharmacological evidence linking CNP/cGMP signaling to microtubule dynamics. We show that low doses of nocodazole that interfere with dynamic microtubules (Fig. 6) abolished both CNP- and cGMP-elicited branch formation (Fig. 7) and CNP-stimulated axon growth (Fig. 8) in the DRG neuron culture [Fig. 9(A)]. The does responses are slightly different at the highest dose (100 nM) tested, as CNP/cGMP-induced branching was inhibited completely to the similar level as the controls [Fig. 7(K–N)], while CNP-stimulated axon growth in explants was not [Fig. 8(I)]. Such difference may suggest that microtubules regulated by CNP/cGMP signaling have different impacts on axon branching and growth. It may also suggest that CNP activation can counteract the inhibitory effect of nocodazole during axon growth.

Since CNP/cGMP signaling is required for bifurcation *in vivo* (Schmidt et al., 2007, 2009; Zhao and Ma, 2009; Zhao et al., 2009), the branching activity we study in culture may reflect a general collateral mechanism as recently proposed (Gibson and Ma, 2011). Following this logic, our result is thus consistent with the role of dynamic microtubules in collateral branching of cortical axon stimulated by Netrin (Dent et al., 2004). It is also consistent with another finding of a similar reduction in axon branching by taxol, which perturbs microtubule dynamics by stabilization (Letourneau et al., 1986). However, our result differs from two past studies, in which

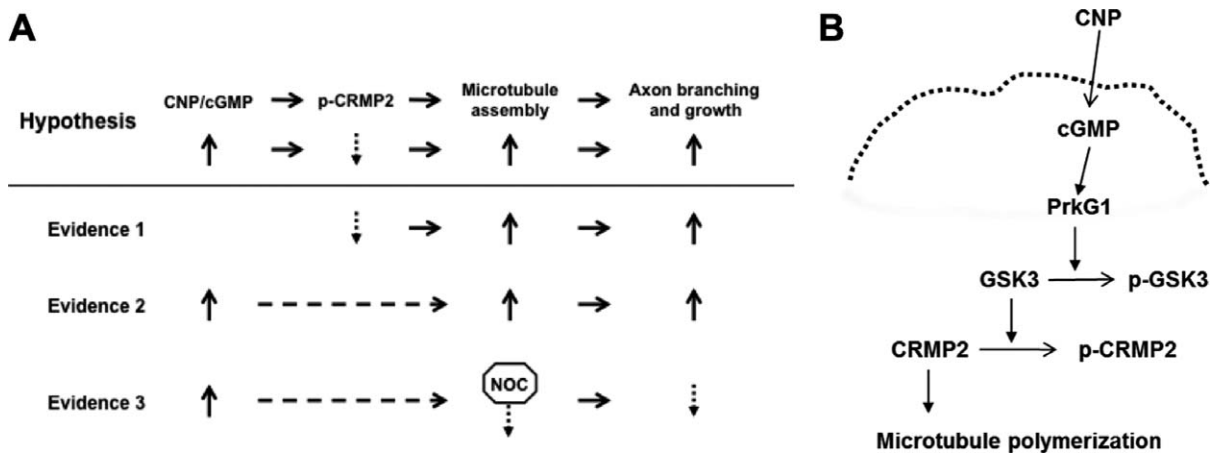

Figure 9 Regulation of microtubule assembly in promoting axon branching and growth by CNP signaling. A) Summary of the hypothesis and the three lines of evidence that support it. Here, activated CNP/cGMP signaling leads to decreased phosphorylation of CRMP2 (p-CRMP2), which activates microtubule assembly and axon branching/growth. The supporting evidence is based on correlative observations from biochemical, cell biological, and pharmacological studies. NOC: nocodazole. B) The proposed molecular pathway connecting the extracellular cue CNP to dynamic microtubule polymerization. Here, CNP binds to its cell surface receptor Npr2, which catalyzes the production of cGMP. cGMP-activated PrkG1 can phosphorylate GSK3 (p-GSK3) and prevent it from phosphorylating CRMP2. Following that in A), decreased CRMP2 phosphorylation (p-CRMP2) then leads to stimulation of microtubule polymerization that is needed for axon branching and growth.

inhibiting microtubule dynamics did not affect spontaneous branch formation in embryonic chick DRG neurons (Gallo and Letourneau, 1999) or even enhanced branch formation in neonatal sympathetic neurons (Baas and Ahmad, 1993). These differences likely result from different culture conditions, especially substrates, used in these studies. For example, our neurons were cultured in the three-dimensional (3D) collagen gel matrix, while the other studies employed two-dimensional (2D) surfaces coated with fibronectin, laminin or poly-ornithine (Letourneau et al., 1986; Baas and Ahmad, 1993; Gallo and Letourneau, 1999). As the cellular responses can be very different under these conditions (Baker and Chen, 2012), branches formed in our 3D cultures or on 2D poly-ornithine (Letourneau et al., 1986) can be sensitive to perturbation of microtubule dynamics, whereas they can still form or even increase production on more permissive 2D substrates (Baas and Ahmad, 1993; Gallo and Letourneau, 1999), perhaps using other mechanisms such as microtubule translocation.

Therefore, our study provides three lines of evidence that jointly support a molecular pathway in which CNP/cGMP activation leads to microtubule assembly during axon branching and growth [Fig. 9(B)]. Although our study points only to the role of dynamic microtubules, it is likely that such regulation also cooperates with microtubule transport and actin dynamics to promote axon growth and branching (Gallo, 2011). In growth cones, dynamic microtubules stimulated by CNP can increase exploration of the space created by actin-led protrusion (Dent and Gertler, 2003; Lowery and Van Vactor, 2009; Dent et al., 2011). Similar changes may occur during branching, when activated CNP/cGMP signaling can increase local microtubule assembly either away from the main growth cone or at a new site along the axon. The resulting microtubule assembly can then help initiate a new growth cone by either increasing local actin dynamics or by stabilizing actin rich protrusion (Schaefer et al., 2008). In addition, increased microtubules assembled locally may allow severing proteins to generate more short microtubules to be transported to the nascent branch thereby promoting branch maturation, a mechanism that is well supported by EM and imaging studies (Yu et al., 1994; Qiang et al., 2010). Thus, dynamic microtubules do not work alone to achieve morphological remodeling needed for axonal development, but can be a key target in branching and growth stimulated by extracellular factors (Kim et al., 2006; Purro et al., 2008).

In conclusion, our current study demonstrates microtubule polymerization as a potential target for CNP/cGMP signaling in regulating axonal development. Our results provide the foundation for

further understanding the cell biological mechanisms of axon branching, growth, and guidance. As a recent study has suggested a role of microtubule stabilization in nerve regeneration (Hellal et al., 2011), our study of microtubule responses to a positive extracellular cue also supports the idea of targeting microtubule assembly to neutralize environmental inhibition of nerve growth in the mammalian central nervous system.

The authors thank members of the Ma lab for helpful discussion, Niels Galjart (Erasmus University) for the EB3-GFP construct, and Virginia Lee (U Penn) for providing the neurofilament antibody. The authors also thank Kathie Eagleson and Steven Tymanskyj for comments on the manuscript.

REFERENCES

Applegate KT, Besson S, Matov A, Bagonis MH, Jaqaman K, Danuser G. 2011. plusTipTracker: Quantitative image analysis software for the measurement of microtubule dynamics. J Struct Biol 176:168–184.

Baas PW, Ahmad FJ. 1993. The transport properties of axonal microtubules establish their polarity orientation. J Cell Biol 120:1427–1437.

Baker BM, Chen CS. 2012. Deconstructing the third dimension: how 3D culture microenvironments alter cellular cues. J Cell Sci 125:3015–3024.

Buck KB, Zheng JQ. 2002. Growth cone turning induced by direct local modification of microtubule dynamics. J Neurosci 22:9358–9367.

Challacombe JF, Snow DM, Letourneau PC. 1997. Dynamic microtubule ends are required for growth cone turning to avoid an inhibitory guidance cue. J Neurosci 17:3085–3095.

Cole AR, Causeret F, Yadirgi G, Hastie CJ, McLauchlan H, McManus EJ, Hernandez F, et al. 2006. Distinct priming kinases contribute to differential regulation of collapsin response mediator proteins by glycogen synthase kinase-3 in vivo. J Biol Chem 281:16591–16598.

Cole AR, Knebel A, Morrice NA, Robertson LA, Irving AJ, Connolly CN, Sutherland C. 2004. GSK-3 phosphorylation of the Alzheimer epitope within collapsin response mediator proteins regulates axon elongation in primary neurons. J Biol Chem 279:50176–50180.

Dent EW, Barnes AM, Tang F, Kalil K. 2004. Netrin-1 and semaphorin 3A promote or inhibit cortical axon branching, respectively, by reorganization of the cytoskeleton. J Neurosci 24:3002–3012.

Dent EW, Gertler FB. 2003. Cytoskeletal dynamics and transport in growth cone motility and axon guidance. Neuron 40:209–227.

Dent EW, Gupton SL, Gertler FB. 2011. The growth cone cytoskeleton in axon outgrowth and guidance. Cold Spring Harb Perspect Biol 3: a001800.

Dent EW, Kalil K. 2001. Axon branching requires interactions between dynamic microtubules and actin filaments. J Neurosci 21:9757–9769.

Fukata Y, Itoh TJ, Kimura T, Menager C, Nishimura T, Shiromizu T, Watanabe H, et al. 2002. CRMP-2 binds to tubulin heterodimers to promote microtubule assembly. Nat Cell Biol 4:583–591.

Gallo G. 2011. The cytoskeletal and signaling mechanisms of axon collateral branching. Dev Neurobiol 71:201–220.

Gallo G, Letourneau PC. 1999. Different contributions of microtubule dynamics and transport to the growth of axons and collateral sprouts. J Neurosci 19:3860–3873.

Garrison AK, Shanmugam M, Leung HC, Xia C, Wang Z, Ma L. 2012. Visualization and analysis of microtubule dynamics using dual color-coded display of plus-end labels PLoS One 7:e50421.

Gibson DA, Ma L. 2011. Developmental regulation of axon branching in the vertebrate nervous system. Development 138:183–195.

Hellal F, Hurtado A, Ruschel J, Flynn KC, Laskowski CJ, Umlauf M, Kapitein LC, et al. 2011. Microtubule stabilization reduces scarring and causes axon regeneration after spinal cord injury. Science 331:928–931.

Hur EM, Zhou FQ. 2010. GSK3 signalling in neural development. Nat Rev Neurosci 11:539–551.

Inagaki N, Chihara K, Arimura N, Menager C, Kawano Y, Matsuo N, Nishimura T, et al. 2001. CRMP-2 induces axons in cultured hippocampal neurons. Nat Neurosci 4:781–782.

Jaworski J, Kapitein LC, Gouveia SM, Dortland BR, Wulf PS, Grigoriev I, Camera P, et al. 2009. Dynamic microtubules regulate dendritic spine morphology and synaptic plasticity. Neuron 61:85–100.

Kim WY, Zhou FQ, Zhou J, Yokota Y, Wang YM, Yoshimura T, Kaibuchi K, et al. 2006. Essential roles for GSK-3s and GSK-3-primed substrates in neurotrophin-induced and hippocampal axon growth. Neuron 52:981–996.

Letourneau PC, Shattuck TA, Ressler AH. 1986. Branching of sensory and sympathetic neurites in vitro is inhibited by treatment with taxol. J Neurosci 6:1912–1917.

Lowery LA, Van Vactor D. 2009. The trip of the tip: Understanding the growth cone machinery. Nat Rev Mol Cell Biol 10:332–343.

Matov A, Applegate K, Kumar P, Thoma C, Krek W, Danuser G, Wittmann T. 2010. Analysis of microtubule dynamic instability using a plus-end growth marker. Nat Methods 7:761–768.

Mitchison T, Kirschner M. 1988. Cytoskeletal dynamics and nerve growth. Neuron 1:761–772.

Potter LR, Abbey-Hosch S, Dickey DM. 2006. Natriuretic peptides, their receptors, and cyclic guanosine monophosphate-dependent signaling functions. Endocr Rev 27:47–72.

Purro SA, Ciani L, Hoyos-Flight M, Stamatakou E, Siomou E, Salinas PC. 2008. Wnt regulates axon behavior through changes in microtubule growth directionality: A new role for adenomatous polyposis coli. J Neurosci 28:8644–8654.

Qiang L, Yu W, Liu M, Solowska JM, Baas PW. 2010. Basic fibroblast growth factor elicits formation of interstitial axonal branches via enhanced severing of microtubules. Mol Biol Cell 21:334–344.

Rochlin MW, Wickline KM, Bridgman PC. 1996. Microtubule stability decreases axon elongation but not axoplasm production. J Neurosci 16:3236–3246.

Schaefer AW, Schoonderwoert VT, Ji L, Mederios N, Danuser G, Forscher P. 2008. Coordination of actin filament and microtubule dynamics during neurite outgrowth. Dev Cell 15:146–162.

Schmidt H, Stonkute A, Juttner R, Koesling D, Friebe A, Rathjen FG. 2009. C-type natriuretic peptide (CNP) is a bifurcation factor for sensory neurons. Proc Natl Acad Sci USA 106:16847–16852.

Schmidt H, Stonkute A, Juttner R, Schaffer S, Buttgereit J, Feil R, Hofmann F, et al. 2007. The receptor guanylyl cyclase Npr2 is essential for sensory axon bifurcation within the spinal cord. J Cell Biol 179:331–340.

Stepanova T, Slemmer J, Hoogenraad CC, Lansbergen G, Dortland B, De Zeeuw CI, Grosveld F, et al. 2003. Visualization of microtubule growth in cultured neurons via the use of EB3-GFP (end-binding protein 3-green fluorescent protein). J Neurosci 23:2655–2664.

Suter DM, Schaefer AW, Forscher P. 2004. Microtubule dynamics are necessary for SRC family kinase-dependent growth cone steering. Curr Biol 14:1194–1199.

Tanaka E, Ho T, Kirschner MW. 1995. The role of microtubule dynamics in growth cone motility and axonal growth. J Cell Biol 128:139–155.

Vasquez RJ, Howell B, Yvon AM, Wadsworth P, Cassimeris L. 1997. Nanomolar concentrations of nocodazole alter microtubule dynamic instability in vivo and in vitro. Mol Biol Cell 8:973–985.

Yoshimura T, Kawano Y, Arimura N, Kawabata S, Kikuchi A, Kaibuchi K. 2005. GSK-3beta regulates phosphorylation of CRMP-2 and neuronal polarity. Cell 120:137–149.

Yu W, Ahmad FJ, Baas PW. 1994. Microtubule fragmentation and partitioning in the axon during collateral branch formation. J Neurosci 14:5872–5884.

Yuasa-Kawada J, Suzuki R, Kano F, Ohkawara T, Murata M, Noda M. 2003. Axonal morphogenesis controlled by antagonistic roles of two CRMP subtypes in microtubule organization. Eur J Neurosci 17:2329–2343.

Zhao Z, Ma L. 2009. Regulation of axonal development by natriuretic peptide hormones. Proc Natl Acad Sci USA 106:18016–18021.

Zhao Z, Wang Z, Gu Y, Feil R, Hofmann F, Ma L. 2009. Regulate axon branching by the cyclic GMP pathway via inhibition of glycogen synthase kinase 3 in dorsal root ganglion sensory neurons. J Neurosci 29:1350–1360.

Zhou FQ, Zhou J, Dedhar S, Wu YH, Snider WD. 2004. NGF-induced axon growth is mediated by localized inactivation of GSK-3beta and functions of the microtubule plus end binding protein APC. Neuron 42:897–912.